

**Estimating the
permafrost-carbon
feedback**

T. Schneider von Deimling
et al.

Estimating the permafrost-carbon feedback on global warming

**T. Schneider von Deimling¹, M. Meinshausen¹, A. Levermann^{1,2}, V. Huber¹,
K. Frieler¹, D. M. Lawrence³, and V. Brovkin^{1,4}**

¹Potsdam Institute for Climate Impact Research, Potsdam, Germany

²Potsdam University, Physics Department, Potsdam, Germany

³Climate and Global Dynamics Division, National Center for Atmospheric Research, Boulder, Colorado, USA

⁴Max Planck Institute for Meteorology, Hamburg, Germany

Received: 1 March 2011 – Accepted: 26 April 2011 – Published: 12 May 2011

Correspondence to: T. Schneider von Deimling (schneider@pik-potsdam.de)

Published by Copernicus Publications on behalf of the European Geosciences Union.

Title Page

Abstract

Introduction

Conclusions

References

Tables

Figures

⏪

⏩

◀

▶

Back

Close

Full Screen / Esc

Printer-friendly Version

Interactive Discussion

Abstract

Thawing of permafrost and the associated release of carbon constitutes a positive feedback in the climate system, elevating the effect of anthropogenic GHG emissions on global-mean temperatures. Multiple factors have hindered the quantification of this feedback, which was not included in the CMIP3 and C⁴MIP generation of AOGCMs and carbon cycle models. There are considerable uncertainties in the rate and extent of permafrost thaw, the hydrological and vegetation response to permafrost thaw, the decomposition timescales of freshly thawed organic material, the proportion of soil carbon that might be emitted as carbon dioxide via aerobic decomposition or as methane via anaerobic decomposition, and in the magnitude of the high latitude amplification of global warming that will drive permafrost degradation. Additionally, there are extensive and poorly characterized regional heterogeneities in soil properties, carbon content, and hydrology. Here, we couple a new permafrost module to a reduced complexity carbon-cycle climate model, which allows us to perform a large ensemble of simulations. The ensemble is designed to span the uncertainties listed above and thereby the results provide an estimate of the potential strength of the permafrost-carbon feedback. For the high CO₂ concentration scenario (RCP8.5), 12–52 PgC, or an extra 3–11 % above projected net CO₂ emissions from land carbon cycle feedbacks, are released by 2100 (68 % uncertainty range). This leads to an additional warming of 0.02–0.11 °C. Though projected 21st century emissions are relatively modest, ongoing permafrost thaw and slow but steady soil carbon decomposition means that, by 2300, more than half of the potentially vulnerable permafrost carbon stock in the upper 3m of soil layer (600–1000 PgC) could be released as CO₂, with an extra 1–3 % being released as methane. Our results also suggest that mitigation action in line with the lower scenario RCP3-PD could contain Arctic temperature increase sufficiently that thawing of the permafrost area is limited to 15–30 % and the permafrost-carbon induced temperature increase does not exceed 0.01–0.07 °C by 2300.

Estimating the permafrost-carbon feedback

T. Schneider von Deimling
et al.

Title Page

Abstract

Introduction

Conclusions

References

Tables

Figures



Back

Close

Full Screen / Esc

Printer-friendly Version

Interactive Discussion



1 Introduction

The climate response to anthropogenic greenhouse gas emissions is markedly influenced by internal earth system feedbacks. Carbon cycle feedbacks (Sitch et al., 2008; Cramer et al., 2001; Friedlingstein et al., 2006) are among the most prominent examples of such internal feedbacks, where an initial increase in temperature triggers a reaction from land biomass and soils that leads to carbon dioxide emissions, which in turn amplifies the warming. The strength of this carbon cycle – climate feedback (γ_L) is generally measured as cumulative carbon release (or reduced uptake) per degree of warming. This average land carbon sensitivity γ_L is $+79 \text{ PgC}/^\circ\text{C}$ across the C⁴MIP generation of carbon cycle models (Friedlingstein et al., 2006) under the high SRES A2 scenario up to 2100. Additional release of carbon from thawed permafrost, referred to as “permafrost-carbon feedback” in the following, would add to this land carbon feedback. At present, the release of additional carbon to the atmosphere as carbon dioxide or methane due to the thawing of permafrost (Lawrence and Slater, 2005) and the subsequent decomposition of the soil organic carbon is not typically represented in carbon cycle models. For example, none of the carbon cycle models participating in C⁴MIP (Friedlingstein et al., 2006) included this feedback.

The carbon feedback from high latitude regions and its importance for the future climate is rather unconstrained, with uncertainties existing in the overall availability and quality of carbon stored in frozen soils, permafrost thawing rates, organic matter decomposition rates and, importantly, the relative proportion of anaerobic decomposition (resulting in CO₂ and CH₄ emissions) versus aerobic decomposition (resulting in CO₂ emissions only). However, the permafrost feedback uncertainties are basically “one-sided”, i.e., the inclusion of the permafrost-carbon feedback will most likely increase future climate impacts (or enhance the mitigation challenge). Although some feedbacks that dampen global warming might be triggered, such as vegetation growth induced by permafrost thaw and nutrients release, there is little reason to believe that the net effect of large-scale permafrost thaw would lower future temperature rise (McGuire et al., 2006).

Estimating the permafrost-carbon feedback

T. Schneider von Deimling
et al.

Title Page

Abstract

Introduction

Conclusions

References

Tables

Figures



Back

Close

Full Screen / Esc

Printer-friendly Version

Interactive Discussion



uncertainties in a probabilistic framework over the century long timescales involved, here until 2300. Thus, our approach intends to synthesize and supplement, not to bypass, the highly resolved and process-based permafrost modeling endeavors.

2.2 Climate carbon-cycle model and simulation setup

5 For investigating the climatic effect of future carbon release from thawing permafrost soils we apply MAGICC6, the latest version of a reduced complexity carbon cycle climate model (see e.g. Wigley and Raper, 2002), described in Meinshausen et al. (2008). MAGICC6's carbon cycle can closely emulate 10 high-complexity carbon cycle models that took part in C⁴MIP (Friedlingstein et al., 2006) with respect to their main carbon
10 pools, fluxes and atmospheric CO₂ concentrations in no-feedback and with-feedback carbon cycle experiments. MAGICC also includes gas-cycle parameterizations for methane, including temperature and OH-dependent lifetimes (Ehhalt et al., 2001).

Emissions from the thawing of permafrost soils, however, have not been taken into account neither in C⁴MIP models nor in MAGICC6. Adding the carbon dioxide and
15 methane emissions from the permafrost module (described in the next section) to MAGICC's gas cycles, and feeding back the respective temperatures at each time step to the permafrost and carbon cycle module allows an integrated and internally consistent analysis.

Here, we use a probabilistic version of MAGICC6, which was calibrated to reflect
20 historical observations of surface air temperatures and ocean heat uptake, as described in Meinshausen et al. (2009). We combine 600 equally likely drawings from the 82-dimensional joint probability distribution for this historically constrained climate model with random drawings of 9 sets of carbon cycle model parameters, as well as random drawings from uniform and independent distributions of 21 parameters in our
25 permafrost module (see Table 1). Each of the 9 carbon cycle parameter sets contains 17 individual parameters to emulate one of the C⁴MIP models, as described in Meinshausen et al. (2008), leaving out the one C⁴MIP model that MAGICC6 is least capable of emulating, IPSL.

Estimating the permafrost-carbon feedback

T. Schneider von Deimling
et al.

Title Page

Abstract

Introduction

Conclusions

References

Tables

Figures

⏪

⏩

◀

▶

Back

Close

Full Screen / Esc

Printer-friendly Version

Interactive Discussion



Estimating the permafrost-carbon feedback

T. Schneider von Deimling
et al.

Title Page

Abstract

Introduction

Conclusions

References

Tables

Figures

⏪

⏩

◀

▶

Back

Close

Full Screen / Esc

Printer-friendly Version

Interactive Discussion



We do not prescribe the RCP8.5 GHGs concentrations, but calculate these dynamically using RCP8.5 emissions, so that added permafrost emissions will have an effect on CO₂ and CH₄ concentrations and simulated temperatures. Thus, we start our analysis from the harmonized set of greenhouse gas, aerosol and tropospheric ozone precursor RCP emissions, as they were used for creating the RCP GHG concentrations (and available here: <http://www.pik-potsdam.de/~mmalte/rcps/>).

In addition to our large ensemble simulations, we perform a single illustrative run with default parameter settings for our permafrost module in order to illustrate the dynamics over century long timescales. For this, we use MAGICC6 settings that are identical to those used for producing the RCP concentration scenarios (Meinshausen et al., 2011). Specifically, MAGICC's carbon cycle is calibrated towards the C⁴MIP Bern2.5CC carbon cycle model, and the climate response parameters reflect a median projection across the CMIP3 AOGCMs. For the permafrost module, we assume default settings as listed in Table 1 (“Default”).

2.3 Permafrost module

Here, we provide a conceptual overview of our simplified permafrost module and its main parameter assumptions (see Table 1), with the Appendix providing a detailed mathematical description. Our permafrost module compartmentalizes the organic carbon of permafrost regions into bins with a similar warming threshold, above which permafrost will start thawing. In our simplified framework, neglecting topology and local climate as well as soil conditions, we call these bins “zonal bands”, given that – generally speaking – the Southernmost permafrost regions of the Northern Hemisphere are likely to start thawing first, and the Northernmost regions last. This spatio-temporal characteristic of permafrost thaw is also seen in process-based modeling studies of permafrost degradation (Zhuang et al., 2006).

We assume the frozen carbon content that is potentially vulnerable to decomposition in the upper 3 m in permafrost soils to be between 600 and 1000 PgC. Our assumption is somewhat lower than recent best-guess estimates of 1024 GtC of top 3 m soil carbon

Estimating the permafrost-carbon feedback

T. Schneider von Deimling
et al.

Title Page

Abstract

Introduction

Conclusions

References

Tables

Figures



Back

Close

Full Screen / Esc

Printer-friendly Version

Interactive Discussion



content in the permafrost zone (Tarnocai et al., 2009; Schuur et al., 2008), as we consider only the fraction of permafrost carbon in perennially frozen ground – which eventually might be released to the atmosphere. A smaller portion of the estimated 1000 Pg carbon pool will always reside in near-surface layers, with expected carbon densities approaching those of non-permafrost soils. By default, we assume this potentially vulnerable permafrost carbon content to be uniformly distributed into 50 zonal bands, while for our uncertainty-based projections (see Sect. 3.2) we vary the carbon content across the latitudinal bands (see Appendix A1). We assume the “Southernmost” band to start thawing at any warming above pre-industrial levels ($T_{\min} = 0^{\circ}\text{C}$), and the “Northernmost” band starting to thaw at an Arctic warming above pre-industrial levels of 8–12°C (see Fig. 1). Several studies have suggested that strong degradation of the surface layers of permafrost soils may occur under such pronounced Arctic warming (Lawrence et al., 2008a, b; Saito et al., 2007; Zhang et al., 2008; Yi et al., 2007; Schaefer et al., 2011).

Our modeling approach is meant to describe gradual permafrost degradation resulting from progressive active layer thickening, but it does not explicitly account for permafrost degradation by talik formation, erosion or thermokarst development – processes also of importance to the fate of future permafrost.

We assume a range of 1.4 to 2.0 for polar amplification, i.e. the average increase of annual average surface air temperatures in the permafrost region relative to the global-mean increase. We base this on an analysis of CMIP3 AOGCM (Meehl et al., 2005) projections, that derives a central estimate of ~ 1.6 with a 2-sigma uncertainty of 0.2 (Frieler et al., 2011). Our upper end of the assumed uniform distribution considered here is slightly above the maximum value from AOGCMs to account for cases of strong future sea ice retreat, which may only partly be captured by the analyzed CMIP3 AOGCMs (Stroeve et al., 2007). Such a strong retreat will increase polar temperature amplification in permafrost regions (Screen and Simmonds, 2010; Lawrence et al., 2008b). For the purpose of retrieving this polar amplification factor from the AOGCMs, the diagnosed permafrost region is here assumed as North-Eastern Europe

(NEE), North-Asia/Siberia (NAS) and Alaska (ALA) following the region definitions of Giorgi et al. (2005).

The two main soil types in permafrost regions – mineral and peatland soils – exhibit rather different properties of relevance to induced emissions (e.g. in terms of thermal soil conductivities or in terms of the ratio of aerobic vs. anaerobic soil conditions). By peatland soils here we understand soils with a high fraction of organic material (peat, litter) which are likely to turn into temporal wetlands when permafrost thaws. We thus subdivide the carbon in each zonal band into four pools: permafrost carbon stored in mineral and in peatland soils, each pool being subdivided into an aerobic and an anaerobic fraction. The largest carbon pool is characterized by physical properties of mineral soils and we assume that these soils contain 70–90 % of the total permafrost carbon content (see R_{ms} in Table 1), given that an estimated 80 % of carbon is stored in the upper 3m frozen mineral soils (Tarnocai et al., 2009).

A key uncertainty is the fraction of carbon that might be decomposed under anaerobic conditions – resulting potentially in methane emissions to the atmosphere. Given the high warming potential of methane, the overall magnitude of the permafrost-carbon feedback will depend strongly on this fraction.

Based on Frolking et al. (2001) we assume an anaerobic fraction of 70 % to 90 % for peatland soils. Mineral soils are dominated by aerobic conditions with only a small fraction of carbon in anaerobic environments (90 %–99 % aerobic fraction assumed). Although there is large uncertainty, Arctic climate change could increase water-logged areas (and hence the anaerobic part of decomposition) due to increased precipitation and associated soil moisture increases as well as thermokarst lake and wetland formation as ice-rich permafrost soils thaw and subside. On the other hand, increased drainage could lead to the opposite effect, even under increased precipitation. In this study, we hence keep the anaerobic area fractions constant.

In the anaerobic areas, not all decomposed carbon will be emitted as methane. Only half of the decomposed carbon in the anaerobic pool is converted to methane, following the process of methanogenesis (Khvorostyanov et al., 2008b). Furthermore, on its

BGD

8, 4727–4761, 2011

Estimating the permafrost-carbon feedback

T. Schneider von Deimling
et al.

Title Page

Abstract

Introduction

Conclusions

References

Tables

Figures

⏪

⏩

◀

▶

Back

Close

Full Screen / Esc

Printer-friendly Version

Interactive Discussion



anoxic decomposition rates in both soil types are adjusted depending on the soil temperatures. Our sampled parameter range corresponds to Q10 values between 2 and 4 for the aerobic and between 2 and 6 for the anaerobic decomposition, accounting for the large uncertainty in temperature sensitivity of soil carbon mobilization (Davidson and Janssens, 2006). The large anaerobic Q10 range expresses the larger uncertainty in temperature sensitivity of anaerobic decomposition (cf. Walter and Heimann, 2000).

Additionally, we assume that oxic decomposition rates are dependent on soil moisture and implemented a simple soil moisture parameterization based on the annual cycle of soil temperature. The close link between soil temperature and soil moisture in our model is motivated by the fact that state-of-the-art climate models consistently show an increase in water availability (i.e. an increase in precipitation minus evaporation) in permafrost regions in a warmer climate (see Fig. 3.5 in IPCC, 2007).

3 Results

3.1 Illustrative run with default parameter settings

To illustrate the dynamics of our simplified modeling framework, we first show results for a single illustrative experiment for the high RCP8.5 scenario and with default parameters (see Table 1). In our model, permafrost starts degrading at the same level of warming in mineral and peatland soils, though it takes longer for the heat anomaly to penetrate into the peatland soil (Fig. 2a, d). By 2050, only the southern latitudinal bands are subject to degradation, while by 2100 a large fraction of the surface permafrost pool is thawed. Degradation of the northernmost permafrost areas only starts in the second half of the 22nd century.

Given the slow timescale of decomposition, permafrost carbon is released only gradually after thawing the surface soils and continues for centuries. The largest contribution to carbon emission comes from the aerobic decomposition of organic material located in the mineral soil pool (Fig. 2b). The peak emissions resulting from aerobic

BGD

8, 4727–4761, 2011

Estimating the permafrost-carbon feedback

T. Schneider von Deimling
et al.

Title Page

Abstract

Introduction

Conclusions

References

Tables

Figures

⏪

⏩

◀

▶

Back

Close

Full Screen / Esc

Printer-friendly Version

Interactive Discussion



Estimating the permafrost-carbon feedback

T. Schneider von Deimling
et al.

Title Page

Abstract

Introduction

Conclusions

References

Tables

Figures

⏪

⏩

◀

▶

Back

Close

Full Screen / Esc

Printer-friendly Version

Interactive Discussion

decomposition of peatland carbon around 2150 is an order of magnitude smaller compared to those from aerobic decomposition from mineral soils (see Fig. 2b, e). This is because of the assumed 20:80 ratio of total peatland to mineral soil carbon, the slower thawing and decomposition rates of peatland soil compared to mineral soils, and the much higher anaerobic soil fraction in peatlands. Carbon release from the anaerobic pool describes the slowest timescale of permafrost dynamics due to the much lower decomposition rates in anaerobic compared to aerobic environments (a factor of ten difference for our default case). Carbon emissions due to aerobic decomposition fall again after peaks in the early 22nd century for the lower zonal bands, indicating depletion of available soil carbon stocks over the multi-centennial timeframe considered here (see Fig. 2b, e).

Assuming that northern peatlands are complex, adaptive ecosystem (Belyea and Baird, 2006) this carbon pool might prove to be less vulnerable to loss due to self-sustaining vegetation and hydrology feedbacks (Frolking et al., 2011). We assume that the majority of this pool is subject to slow anaerobic decomposition, which is tantamount to assuming a larger resilience of peatland carbon to climate change.

3.2 Projections for RCPs including uncertainties

In the following, we go beyond a consideration of our default parameter scenario and discuss model outcomes in the probabilistic framework in which we account for uncertainty in parameters of the carbon-cycle climate model and in the permafrost module (see Table 1).

For the mitigation scenario RCP3-PD that limits global mean temperature changes to below 2 °C, cumulative CO₂ emissions from permafrost are 4 PgC (68 % uncertainty range: 2–7 PgC) by 2100 (Table 2). The analysis of RCP8.5, a scenario that implies extensive global warming reaching well above 10 °C by 2150 (Fig. 3e), shows a pronounced degradation of near-surface permafrost (about 31–66 % thaw, 68 % uncertainty range) by 2100 and almost complete thawing by 2200. Modeling studies based on physical permafrost schemes consistently show pronounced permafrost

concentration change from permafrost carbon is above our high-end estimate in 2100 (22 ppm for the upper 68 %-range, RCP8.5, see Table 2). A recent study by Schaefer et al. (2011) infers a cumulative carbon flux of 190 ± 64 Gt from thawed permafrost by 2200 based on the A1B scenario. Our simulation results based on the RCP6 scenario (describing a forcing of comparable magnitude) suggest median emissions until 2200 of 69 GtC, with maximum emission of 146 GtC for the 68 % range (245 GtC for the 90 % range). Key to the higher estimates of Schaefer et al. (2011) is their simulated fast permafrost degradation leading to 80–90 % of permafrost carbon thaw before 2100 (while we infer an upper bound of 54 % permafrost loss for the 90 % uncertainty range by 2100, RCP6). Slow decomposition of anaerobic pools and slow degradation of peatland soils is not accounted for in their study. Much lower C emission is suggested by (Zhuang et al., 2006) who applied a process-based emission model to infer an upper estimate of 17 PgC resulting from permafrost thaw in the 21st century for their high emission scenario (being slightly larger than RCP8.5).

Our inferred methane emissions from anaerobic decomposition of permafrost carbon are rather small, accounting for approximately 1 % to 3 % of the total carbon release. Due to the higher radiative forcing efficiency of methane, this relatively low fractional release of methane is important with respect to the total temperature increase, with up to a third of the permafrost-induced forcing stemming from these methane releases under the high RCP8.5 scenario (cf. Table 2). Compared to current total anthropogenic methane emissions (roughly $300 \text{ MtCH}_4 \text{ yr}^{-1}$ in yr 2000), permafrost-induced methane emissions can reach a similar magnitude by 2200 (median around $100 \text{ MtCH}_4 \text{ yr}^{-1}$, see Fig. 3b), which corresponds to roughly a factor of 3 to 10 increase of 20th century natural net methane emissions from the Arctic (McGuire et al., 2009).

If the Siberian Yedoma complex were to thaw as analysed by one modeling study which factored in the heat release by microbial decomposition (Khvorostyanov et al., 2008a) – a process which we neglect in our considerations – permafrost CH_4 release rates are likely to strongly increase. Future methane emission up to $30\,000 \text{ TgCH}_4$ is estimated from a complete thawing of the Yedoma carbon pool alone, based on

Estimating the permafrost-carbon feedback

T. Schneider von Deimling
et al.

[Title Page](#)[Abstract](#)[Introduction](#)[Conclusions](#)[References](#)[Tables](#)[Figures](#)[Back](#)[Close](#)[Full Screen / Esc](#)[Printer-friendly Version](#)[Interactive Discussion](#)

up-scaling of observational estimates from extensive hotspot methane ebullition over thermokarst lakes (Walter et al., 2006, 2007b).

Our global-mean temperature simulations of the RCP scenarios, once including the permafrost module and once excluding it, indicate that the median warming by 2100 is not substantially altered. If we accounted for rather high rates of permafrost thaw as modeled by (Lawrence et al., 2008a) and (Schaefer et al., 2011) we expect to infer a non-negligible warming contribution by 2100 from permafrost carbon for the high anthropogenic emission scenarios. For the mitigation scenario RCP3-PD, permafrost-carbon feedbacks add negligibly to the warming. For the high RCP8.5 scenario, permafrost-carbon feedbacks can trigger additional global-mean temperature increase of about 0.05 °C (0.02–0.11 °C) by 2100, further increasing to 0.40 °C (0.17–0.94 °C) by 2200 and 0.58 °C (0.30–1.15 °C) in 2300 (see Table 2 and Fig. 3f). The intermediate RCP scenarios imply intermediate permafrost feedbacks, roughly proportional to their radiative forcing levels (see Table 2).

3.3 Permafrost sensitivities

The permafrost carbon pool is diminished by 5.1 PgC (2.7–8.6 PgC) per degree of global warming under RCP8.5. This is the RCP scenario that is most closely comparable to the SRES A2 scenario, for which the C⁴MIP intercomparison has been undertaken. Hence, the total carbon sensitivity of, on average, 79 PgC/°C with a broad range from 20 to 177 PgC/°C across the C⁴MIP models (Friedlingstein et al., 2006) could be slightly higher. When permafrost-carbon feedbacks are included, the average estimate would increase 6% (3% to 10%), shifting the best estimate of total land carbon sensitivity from 79 PgC/°C by 2100 to above 84 PgC/°C.

Our results highlight the limitations of this indicator “carbon pool sensitivity”, given that cumulative carbon releases per degree of warming is not a scenario- or time-independent characteristic (Table 2). Until 2100, the permafrost-carbon sensitivity under the lower scenarios, RCP3-PD, RCP4.5 and RCP6 is only estimated to be half of that under RCP8.5. On longer timescales, the permafrost-carbon sensitivity increases

Estimating the permafrost-carbon feedback

T. Schneider von Deimling
et al.

Title Page

Abstract

Introduction

Conclusions

References

Tables

Figures

⏪

⏩

◀

▶

Back

Close

Full Screen / Esc

Printer-friendly Version

Interactive Discussion



substantially, 5 times under RCP3-PD until 2300 and approximately 10 times under the higher RCP6 and RCP8.5 (see Table 2).

4 Limitations

The robustness of our results crucially depends on our assumptions made for parameterizing physical and microbial processes which determine the magnitude and timing of carbon release from permafrost soils. By having generously varied model parameters to account for known uncertainties we have spanned a broad possible range of future permafrost evolution. Yet our simplified representation of complex permafrost thawing dynamics and subsequent carbon release has several important limitations.

Effects of snow cover changes, which either can amplify or dampen soil warming, are not accounted for explicitly in our model. While snow state changes are likely to have strongly impacted recent soil temperatures trends, its role of affecting soil temperatures beyond 2050 is expected to exert a much smaller weight as surface air warming becomes the dominant driver for permafrost degradation (Lawrence and Slater, 2010).

Due to pronounced spatial inhomogeneities in the soils and in local climatology, the “real world” change at specific permafrost sites will differ strongly from our simplified model which assumes that carbon is distributed homogeneously in each latitudinal band and is of the same quality (while carbon content is varied across latitudes). Highly site-specific permafrost thaw can result from site-specific soil and vegetation cover properties, such as a strong insulation effect exerted by an organic-rich surface or a thin peat layer, or the effect on soil thermal properties resulting from unfrozen water in the ground (Yi et al., 2007; Nicolsky et al., 2007). Additionally, interaction of the C- and N-cycle (Canadell et al., 2007) and various non-linear and complex ecosystem feedback loops (Heimann and Reichstein, 2008; Jorgenson et al., 2010) can play an important role in the fate of permafrost carbon but are not considered here.

Estimating the permafrost-carbon feedback

T. Schneider von Deimling
et al.

Title Page

Abstract

Introduction

Conclusions

References

Tables

Figures



Back

Close

Full Screen / Esc

Printer-friendly Version

Interactive Discussion



Estimating the permafrost-carbon feedback

T. Schneider von Deimling
et al.

[Title Page](#)[Abstract](#)[Introduction](#)[Conclusions](#)[References](#)[Tables](#)[Figures](#)[Back](#)[Close](#)[Full Screen / Esc](#)[Printer-friendly Version](#)[Interactive Discussion](#)

We focus our analysis on the top 3 m of land permafrost soils where carbon densities are high and uncertainty about the rate of thaw of deep ground layers is not as important. For large warming anomalies on multi-centennial timescales, carbon release from deeper carbon reservoirs is likely. Of particular relevance is the potential degradation and emissions of highly labile carbon found in deeper layers of the Siberian Yedoma complex (Khvorostyanov et al., 2008a) and fluvial deposits (Tarnocai et al., 2009), with a potential to further increase emissions from permafrost. Furthermore, large amounts of carbon are likely to be stored in sub-sea permafrost (Shakhova et al., 2010a) and in methane hydrate deposits on continental margins (Archer et al., 2009). We did not account for these additional carbon sources and therefore our high-end estimate of 1000 PgC of carbon being potentially vulnerable to future release is likely a conservative estimate.

A key question remains with respect to the impact of permafrost thaw on water table depth, which ultimately determines the fraction of carbon released as CO₂ or as methane. This aspect is considered an obvious gap in state-of-the-art Earth system models (O'Connor et al., 2010). Thawing may lead to enhanced soil drainage (lowering of water table) while landscape collapse is likely to favor thermokarst lake or wetland formation, resulting in increased CH₄/CO₂ emission ratios. High rates of CH₄ release from newly forming thermokarst lakes indicate that this process might be a crucial contributor to future methane emission from permafrost soils (Walter et al., 2007a). Apart from this effect on hydrology, soil thermal properties are changed with enhanced permafrost thaw, although this dynamic is not considered in our study.

With future permafrost thaw and Arctic temperature rise, vegetation cover will respond to more favorable growing conditions, resulting in expected higher CO₂ sequestration in Arctic regions (Canadell et al., 2007; Friedlingstein et al., 2006). Nutrients, released during the decomposition of organic material, could support new forest and biomass buildup. We do not explicitly account for the effect of increased CO₂ uptake by expansion of vegetation into thawed permafrost regions. From a radiative balance viewpoint, the carbon sequestration effect is likely to be compensated somewhat or

in full by the lowering of albedo resulting from modified Arctic vegetation (Matthews and Keith, 2007; Betts, 2000). In case of very strong warming with a pronounced decrease in spring-time snow-cover this compensation will be less effective (a decrease in albedo feedback) – while increased transpiration from enhanced forest cover and the associated positive water vapor feedback might become more important (Swann et al., 2010).

Our results are limited by the realism of global-mean temperature projections: While our results cannot confidently project warmings of 10 °C, which is above the upper end of the AOGCM calibration range of MAGICC6 (approximately 6 °C), our results can be taken as an indication of the timing and potential magnitude of permafrost feedback effects. The results that we present here, i.e. that permafrost-carbon feedbacks are relevant at the global scale and will become increasingly important on longer time horizons, are based on highly simplified representations of permafrost and carbon-cycle climate dynamics. Similar studies using process-based models that are constrained by observations are urgently needed to better quantify permafrost-carbon and other permafrost feedbacks more robustly.

5 Conclusions

The inclusion of a highly simplified, dynamic permafrost module into the reduced complexity carbon-cycle climate model MAGICC has shown how permafrost carbon emissions could affect long-term projections of future temperature change. Our results underline the importance of analyzing long-term consequences of land carbon emissions beyond 2100. Studies focusing on short time horizons (e.g. Anisimov, 2007) infer a rather small permafrost feedback, in line with our results, while climatic consequences of thawing permafrost soils become clearly apparent after 2100 for the medium and higher RCP scenarios. Even more pronounced than many other components of the Earth System, the permafrost feedback highlights the inert and slow response to human perturbations. Once unlocked under strong warming, thawing and decomposition

BGD

8, 4727–4761, 2011

Estimating the permafrost-carbon feedback

T. Schneider von Deimling
et al.

Title Page

Abstract

Introduction

Conclusions

References

Tables

Figures



Back

Close

Full Screen / Esc

Printer-friendly Version

Interactive Discussion



total permafrost carbon might be subject to thawing for comparatively low temperature increases, we introduced flexibility in the model regarding this initial carbon distribution along the “North-South” axis. Depending on the input parameter φ , initial total carbon pool C_0 is distributed across our n zonal bands $C_{i,0}$ according to:

$$C_{i,0} = \begin{cases} \left(i \frac{|\varphi|}{n^2} + \frac{1-|\varphi|}{n} \right) \frac{1}{A_{\text{tot}}} C_0, & -1 \leq \varphi < 0 \\ \frac{1}{n} C_0, & \varphi = 0 \\ \left((n-i+1) \frac{|\varphi|}{n^2} + \frac{1-|\varphi|}{n} \right) \frac{1}{A_{\text{tot}}} C_0, & 0 < \varphi \leq 1 \end{cases} \quad (\text{A1})$$

with A_{tot} being the normalization constant, ensuring that the individual contributions add up to C_0 (surface area of the grey shaded region marked in Fig. A1), ($A_{\text{tot}} = 1 - \frac{|\varphi|}{2}(1 - \frac{1}{n})$). For the limit $\varphi = 1$, the “northernmost” zonal band ($i = n$) will only contain the small fraction $1/(n^2 \cdot A_{\text{tot}})$ of the total carbon pool, while the southernmost zonal band ($i = 1$) will contain the largest fraction $1/(n \cdot A_{\text{tot}})$ with linear increasing carbon pool fractions in between. Graphically, the carbon pool fraction distributions that can be set via the φ parameter can be represented by a horizontally striped trapeze, with the lower/upper parallel side approaching zero for φ being set at 1 or -1 (see Fig. A1). This initial carbon pool in each zonal band is attributed to the mineral and peatland soil fractions using the parameters $R_{\text{ms,south}}$ for band $i = 1$ and $R_{\text{ms,north}}$ for the “northernmost” band $i = n$, with linear interpolation for intermediate zonal bands.

A2 The thawing threshold in each zonal band

A regional warming threshold $\Delta T_i^{\text{thresh}}$ is attributed to each zonal band for describing the latitudinal dependency of permafrost thaw. A minimum warming for thaw is required in the Southernmost band (ΔT_{min}), and a maximum warming threshold in the Northernmost band (ΔT_{max}). Thus, by linearly interpolating between the zonal bands, the warming threshold in zonal band i is defined as:

$$\Delta T_i^{\text{thresh}} = \Delta T_{\text{min}} + \frac{(i-1)(\Delta T_{\text{max}} - \Delta T_{\text{min}})}{n-1} \quad (\text{A2})$$

Estimating the permafrost-carbon feedback

T. Schneider von Deimling
et al.

Title Page

Abstract

Introduction

Conclusions

References

Tables

Figures

⏪

⏩

◀

▶

Back

Close

Full Screen / Esc

Printer-friendly Version

Interactive Discussion



Using this threshold, we calculate the maximum temperature reached during summer ($T_{i,t}^{\text{summer}}$) relative to the freezing point in each year t in each zonal band:

$$T_{i,t}^{\text{summer}} = \alpha \Delta T_{\text{global},t} - \Delta T_i^{\text{thresh}} \quad (\text{A3})$$

with $\Delta T_{\text{global},t}$ being the global-mean, annual average temperature anomaly, α being the latitudinal amplification factor, i.e., the ratio at which permafrost regions are expected to warm relative to the global mean, assuming a linear relationship between regional and global warming (Santer et al., 1990; Mitchell, 2003; Frieler et al., 2011). As soon as global temperature increase is high enough to raise permafrost summer temperatures above zero in a given latitudinal band, permafrost thaw is initiated and soil carbon in this band gets subject to decomposition.

We calculate the transformation from soil between the permafrost and non-permafrost area on an annual basis. The summer temperature in year t is simply multiplied with the thawing/refreezing rate β_x to calculate the thawing or re-freezing fractional depth D_t^x of each zonal band, with ($D_t^x = \beta_x T_{i,t}^{\text{summer}}$ (x denoting either “ms” or “peat” for the mineral or peatland soils)). By choosing different settings for β_x , we account for the large uncertainty present in model simulations of permafrost thaw.

A3 Decomposition rates and their sensitivities to soil moisture and temperature

Oxic decomposition rates in peat and mineral soils are assumed to be dependent on two factors, i.e., soil moisture and soil temperature. In the following, we describe simple parametrizations of the soil moisture status and of the temperature dependency of decomposition to infer a formula for effective decomposition rates. For anoxic conditions, decomposition rates are a function of soil temperature only.

Using a simple sinusoidal function, we approximate the annual cycle of the effective soil temperature in each band i , to compute the monthly soil temperatures $T_{i,m}^{\text{soil}}$

$$T_{i,m}^{\text{soil}} = \frac{\Phi}{2} \sin \frac{\pi(m-1)}{11} - \frac{\Phi}{2} + T_{i,t}^{\text{summer}} \quad (\text{A4})$$

Estimating the permafrost-carbon feedback

T. Schneider von Deimling
et al.

Title Page

Abstract

Introduction

Conclusions

References

Tables

Figures

⏪

⏩

◀

▶

Back

Close

Full Screen / Esc

Printer-friendly Version

Interactive Discussion



with $m = 1, \dots, 12$ denoting the 12 months of year t , and Φ the amplitude of the mean soil temperature cycle in the upper 3 m (estimated as 4–6 °C) (cf. Khvorostyanov et al., 2008b).

Building on the monthly soil temperatures in each latitudinal band, we linearly approximate the temperature dependency of soil moisture $W_{i,m}^{\text{soil}}$ according to model results from a $4 \times \text{CO}_2$ run of the LPJ model (Sitch et al., 2003):

$$W_{i,m}^{\text{soil}} = \begin{cases} W_{\min}, & m_{\text{T}} T_{i,m}^{\text{soil}} + W_{\text{off}} \leq W_{\min} \\ m_{\text{T}} T_{i,m}^{\text{soil}} + W_{\text{off}}, & m_{\text{T}} T_{i,m}^{\text{soil}} + W_{\text{off}} > W_{\min} \end{cases} \quad (\text{A5})$$

with m_{T} determining the soil moisture temperature sensitivity (default of 0.04 °C⁻¹). Following Wania et al. (2009), we describe the moisture modifier function $F(W)$ as:

$$F(W_{i,m}^{\text{soil}}) = \frac{1 - e^{-W_{i,m}^{\text{soil}}}}{1 - e^{-1}} \quad (\text{A6})$$

The temperature dependence of autotrophic respiration is described by a modified Arrhenius equation (Lloyd and Taylor, 1994; Sitch et al., 2003):

$$F(T_{i,m}^{\text{soil}}) = e^{\lambda \left(\frac{1}{56.02} - \frac{1}{T_{i,m}^{\text{soil}} + 46.02} \right)} \quad (\text{A7})$$

with λ describing the activation energy and $F(T = 20^\circ\text{C})$ often being called the “Q10” factor, representing the increase in the decomposition rate from 10 °C to 20 °C.

Using results from Eqs. (A6) and (A7), the annual average decomposition rate $\theta_{t,i,\text{aer}}^{\text{ms}}$ for aerobic respiration in mineral soils is derived from the inverse turnover time $1/\tau_{\text{aer}}^{\text{ms}}$ and modulated by the soil temperature modifier $F(T)$ and the moisture modifier $F(W)$. The time- and zonal band dependent decomposition rate $\theta_{t,i,\text{aer}}^{\text{ms}}$ for the mineral soil type and aerobic decomposition segment is the annual average over monthly decomposition rates:

$$\tau_{t,i,\text{aer}}^{\text{ms}} = \frac{1}{\tau_{\text{aer}}^{\text{ms}}} F(T_{i,m}^{\text{soil}}) F(W_{i,m}^{\text{soil}}) \quad (\text{A8})$$

Estimating the permafrost-carbon feedback

T. Schneider von Deimling et al.

Title Page

Abstract

Introduction

Conclusions

References

Tables

Figures

◀

▶

◀

▶

Back

Close

Full Screen / Esc

Printer-friendly Version

Interactive Discussion



The effective aerobic decomposition rates for peatland carbon pool fractions are assumed to be lower, proportional to $\theta_{t,i,aer}^{ms}$ using the proportionality factors $R_{peat/ms}$ (assumed range 0.3 to 0.7). Anaerobic decomposition is calculated by using Eq. (A8) with a fixed soil moisture modifier ($F(W_{i,m}^{soil}) = 1$) and an aerobic to anaerobic proportionality factor $R_{an/aer}$ with a default value of 0.1.

A4 Area of aerobic and anaerobic decomposition

The anaerobic area fraction A_{an}^x (for peatland or mineral soils) relates to the thawed permafrost area, so that the anaerobic area fraction $A_{t,i,an}^x$ in relation to the total zonal band area (indicated by the hyphen) is given by

$$A_{t,i,an}^x = A_{an}^x \left(1 - A_{t,i,pf}^x\right) \quad (A9)$$

with $A_{t,i,pf}^x$ being the fraction of intact permafrost, starting at 100 % at the beginning of the simulations and then decreasing as warming progresses.

Unlike in a spatially resolved high resolution permafrost model coupled to an AOGCM, our simplified structure does not permit to keep track of the carbon content of individual soil patches over time. Thus, for a change in the permanently frozen area fraction, an assumption is required of how much carbon is actually transferred between the respective carbon pools. We make a simplifying assumption of a uniformly distributed carbon density in each area type, anaerobic and aerobic, permafrost and non-permafrost. Ideally, a higher resolved model would keep track of individual patches or parts of the permafrost column. Thus, the change of the thawed anaerobic ($z = \text{“an”}$) or aerobic ($z = \text{“aer”}$) area $\Delta A_{t,i,z}^x$ relative to the total zonal band area is given by the annual thawing rate D_t^x and the respective permafrost area $A_{t,i,pf}^x$

$$\Delta A_{t,i,z}^x = D_t^x A_{t,i,pf}^x \quad (A10)$$

In parallel to the fractional areas, the respective carbon pools $C_{t,i,z}^x$ are updated, (i.e. the released carbon is subtracted from the pool) for both soil types x , i.e., peatland and

BGD

8, 4727–4761, 2011

Estimating the permafrost-carbon feedback

T. Schneider von Deimling
et al.

Title Page

Abstract

Introduction

Conclusions

References

Tables

Figures

◀

▶

◀

▶

Back

Close

Full Screen / Esc

Printer-friendly Version

Interactive Discussion



mineral soil, each year t , zonal band i and the anaerobic and aerobic decomposition segments z .

A5 Calculating emissions

The carbon release can now be calculated using the decomposition rates derived in Eq. (A8) above and the calculated amount of thawed carbon being available in the four soil pools (mineral and peatland soil, under aerobic and anaerobic conditions). Given that pools in MAGICC are generally end of year t /beginning of year $t + 1$ quantities, and emissions the sum over year t , the carbon emissions from the aerobic and anaerobic carbon pools are derived as:

$$E_{t,i,z}^x = \theta_{t,i,z}^x C_{t,i,z}^x \quad (\text{A11})$$

Carbon emissions from aerobic decomposition occur in the form of carbon dioxide, and those from the anaerobic decomposition in the form of both methane and carbon dioxide. With half of the carbon in anaerobic areas being converted to CH_4 in the soil, a certain fraction χ of the latter half is assumed to be oxidized on its way through the upper soil layers, before reaching the atmosphere.

Acknowledgements. The authors wish to thank our colleagues whose input was crucial for building our simplified permafrost module. Our special thank is to Vladimir Romanovsky and Alexey Eliseev for discussing physics of permafrost soil thaw, to Charles Tarnocai for discussions about soil carbon characteristics, and to Sybill Schaphoff and Ursula Heyder for their input about dynamic carbon and vegetation modeling. Malte Meinshausen and Katja Frieler were supported by the Federal Environment Agency for Germany (UBA) under project UFO-PLAN FKZ 370841103.

References

Allen, M. R., Frame, D. J., Huntingford, C., Jones, C. D., Lowe, J. A., Meinshausen, M., and Meinshausen, N.: Warming caused by cumulative carbon emissions towards the trillionth tonne, *Nature*, 458, 1163, doi:10.1038/nature08019, 2009.

Estimating the permafrost-carbon feedback

T. Schneider von Deimling
et al.

Title Page

Abstract

Introduction

Conclusions

References

Tables

Figures

⏪

⏩

◀

▶

Back

Close

Full Screen / Esc

Printer-friendly Version

Interactive Discussion



Estimating the permafrost-carbon feedback

T. Schneider von Deimling
et al.

Title Page

Abstract

Introduction

Conclusions

References

Tables

Figures

⏪

⏩

◀

▶

Back

Close

Full Screen / Esc

Printer-friendly Version

Interactive Discussion

Anisimov, O. A.: Potential feedback of thawing permafrost to the global climate system through methane emission, *Environ. Res. Lett.*, 2, 045016, doi:10.1088/1748-9326/2/4/045016, 2007.

Archer, D., Buffett, B., and Brovkin, V.: Ocean methane hydrates as a slow tipping point in the global carbon cycle, *Proceedings of the National Academy of Sciences of the United States of America*, 106, 20596–20601, 2009.

Betts, R. A.: Offset of the potential carbon sink from boreal forestation by decreases in surface albedo, *Nature*, 408, 187–190, 2000.

Canadell, J. G., Pataki, D. E., Pitelka, L. F., Canadell, J., Pataki, D., Gifford, R., Houghton, R., Luo, Y., Raupach, M., Smith, P., and Steffen, W.: Saturation of the Terrestrial Carbon Sink, in: *Terrestrial Ecosystems in a Changing World, Global Change – The IGBP Series*, Springer Berlin Heidelberg, 59–78, 2007.

Cramer, W., Bondeau, A., Woodward, F. I., Prentice, I. C., Betts, R. A., Brovkin, V., Cox, P. M., Fisher, V., Foley, J. A., Friend, A. D., Kucharik, C., Lomas, M. R., Ramankutty, N., Sitch, S., Smith, B., White, A., and Young-Molling, C.: Global response of terrestrial ecosystem structure and function to CO₂ and climate change: results from six dynamic global vegetation models, *Glob. Change Biol.*, 7, 357–373, 2001.

Davidson, E. A. and Janssens, I. A.: Temperature sensitivity of soil carbon decomposition and feedbacks to climate change, *Nature*, 440, 165–173, 2006.

Ehhalt, D., Prather, M. J., Dentener, F., Derwent, R. G., Dlugokencky, E., Holland, E., Isakson, I. S. A., Katima, J., Kirchhoff, V., Matson, P., Midgley, P., and Wang, M.: Atmospheric Chemistry and Greenhouse Gases, in: *Climate Change 2001: The Scientific Basis*, edited by: Houghton, J. T., Ding, Y., Griggs, D. J., Noguer, M., van der Linden, P. J., Dai, X., Maskell, K., and Johnson, C. A., Cambridge University Press, Cambridge, UK, 892, 2001.

Eliseev, A. V., Arzhanov, M. M., Demchenko, P. F., and Mokhov, I. I.: Changes in climatic characteristics of Northern Hemisphere extratropical land in the 21st century: Assessments with the IAP RAS climate model, *Izv. Atmos. Ocean. Phys.*, 45, 271–283, 2009.

Euskirchen, E. S., McGuire, A. D., Kicklighter, D. W., Zhuang, Q., Clein, J. S., Dargaville, R. J., Dye, D. G., Kimball, J. S., McDonald, K. C., Melillo, J. M., Romanovsky, V. E., and Smith, N. V.: Importance of recent shifts in soil thermal dynamics on growing season length, productivity, and carbon sequestration in terrestrial high-latitude ecosystems, *Glob. Change Biol.*, 12, 731–750, 2006.

Friedlingstein, P., Cox, P., Betts, R., Bopp, L., Von Bloh, W., Brovkin, V., Cadule, P., Doney, S.,

Estimating the permafrost-carbon feedback

T. Schneider von Deimling
et al.

Title Page

Abstract

Introduction

Conclusions

References

Tables

Figures

⏪

⏩

◀

▶

Back

Close

Full Screen / Esc

Printer-friendly Version

Interactive Discussion

Eby, M., Fung, I., Bala, G., John, J., Jones, C., Joos, F., Kato, T., Kawamiya, M., Knorr, W., Lindsay, K., Matthews, H. D., Raddatz, T., Rayner, P., Reick, C., Roeckner, E., Schnitzler, K. G., Schnur, R., Strassmann, K., Weaver, A. J., Yoshikawa, C., and Zeng, N.: Climate-carbon cycle feedback analysis: Results from the (CMIP)-M-4 model intercomparison, *J. Climate*, 19, 3337–3353, 2006.

Frieler, K., Meinshausen, M., Braun, N., and Hare, B.: A scaling approach to probabilistic assessment of regional climate change, *J. Climate*, submitted, 2011.

Frolking, S., Roulet, N. T., Moore, T. R., Richard, P. J. H., Lavoie, M., and Muller, S. D.: Modeling northern peatland decomposition and peat accumulation, *Ecosystems*, 4, 479–498, 2001.

Frolking, S., Talbot, J., Roulet, N., Jones, M., Treat, C., Boone Kauffman, B., and Tuittila, E.: Peatlands in the Earth's 21st century coupled climate-carbon system, *Environ. Rev.*, submitted, 2011.

Giorgi, F.: Interdecadal variability of regional climate change: implications for the development of regional climate change scenarios, *Meteorol. Atmos. Phys.*, 89, 1–15, 2005.

Heimann, M. and Reichstein, M.: Terrestrial ecosystem carbon dynamics and climate feedbacks, *Nature*, 451, 289–292, 2008.

IPCC: Climate Change 2007: Synthesis Report. Contribution of Working Groups I, II and III to the Fourth Assessment, 2007.

Report of the Intergovernmental Panel on Climate Change Geneva, Switzerland, 104, 2007.

Jorgenson, M. T., Romanovsky, V., Harden, J., Shur, Y., O'Donnell, J., Schuur, E. A. G., Kanevskiy, M., and Marchenko, S.: Resilience and vulnerability of permafrost to climate change, *Can. J. Forest Res.*, 40, 1219–1236, 2010.

Khorostyanov, D. V., Ciais, P., Krinner, G., and Zimov, S. A.: Vulnerability of east Siberia's frozen carbon stores to future warming, *Geophys. Res. Lett.*, 35, L10703, doi:10.1029/2008GL033639, 2008a.

Khorostyanov, D. V., Krinner, G., Ciais, P., Heimann, M., and Zimov, S. A.: Vulnerability of permafrost carbon to global warming. Part I: model description and role of heat generated by organic matter decomposition, *Tellus B*, 60, 250–264, 2008b.

Lawrence, D. M. and Slater, A. G.: A projection of severe near-surface permafrost degradation during the 21st century, *Geophys. Res. Lett.*, 32, L24401, doi:10.1029/2005GL025080, 2005.

Lawrence, D. M., Slater, A. G., Romanovsky, V. E., and Nicolsky, D. J.: Sensitivity of a model projection of near-surface permafrost degradation to soil column depth and representation

Estimating the permafrost-carbon feedback

T. Schneider von Deimling
et al.

Title Page

Abstract

Introduction

Conclusions

References

Tables

Figures

⏪

⏩

◀

▶

Back

Close

Full Screen / Esc

Printer-friendly Version

Interactive Discussion



of soil organic matter, *J. Geophys. Res.-Earth*, 113, F02011, doi:10.1029/2007JF000883, 2008a.

Lawrence, D. M., Slater, A. G., Tomas, R. A., Holland, M. M., and Deser, C.: Accelerated Arctic land warming and permafrost degradation during rapid sea ice loss, *Geophys. Res. Lett.*, 35, L11506, doi:10.1029/2008GL033985, 2008b.

Lawrence, D. M. and Slater, A. G.: The contribution of snow condition trends to future ground climate, *Clim. Dynam.*, 34, 969–981, 2010.

Lloyd, J. and Taylor, J. A.: On the Temperature-Dependence of Soil Respiration, *Funct. Ecol.*, 8, 315–323, 1994.

Matthews, H. D. and Keith, D. W.: Carbon-cycle feedbacks increase the likelihood of a warmer future, *Geophys. Res. Lett.*, 34, L09702, doi:10.1029/2006GL028685, 2007.

McGuire, A. D., Chapin, F. S., Walsh, J. E., and Wirth, C.: Integrated Regional Changes in Arctic Climate Feedbacks: Implications for the Global Climate System*, *Annu. Rev. Env. Resour.*, 31, 61–91, doi:10.1146/annurev.energy.31.020105.100253, 2006.

McGuire, A. D., Anderson, L. G., Christensen, T. R., Dallimore, S., Guo, L. D., Hayes, D. J., Heimann, M., Lorenson, T. D., Macdonald, R. W., and Roulet, N.: Sensitivity of the carbon cycle in the Arctic to climate change, *Ecol. Monogr.*, 79, 523–555, 2009.

Meehl, G. A., Covey, C., McAvaney, B., Latif, M., and Stouffer, R. J.: Overview of coupled model intercomparison project, *Bulletin of the American Meteorological Society (BAMS)*, 86, 89–93, 2005.

Meinshausen, M., Raper, S. C. B., and Wigley, T. M. L.: Emulating coupled atmosphere-ocean and carbon cycle models with a simpler model, *MAGICC6 – Part 1: Model description and calibration*, *Atmos. Chem. Phys.*, 11, 1417–1456, doi:10.5194/acp-11-1417-2011, 2011.

Meinshausen, M., Meinshausen, N., Hare, W., Raper, S. C. B., Frieler, K., Knutti, R., Frame, D. J., and Allen, M. R.: Greenhouse-gas emission targets for limiting global warming to 2 degrees C, *Nature*, 458, 1158–1163, doi:10.1038/nature08017, 2009.

Meinshausen, M., Smith, S. J., Calvin, K. V., Daniel, J. S., Kainuma, M. L. T., Lamarque, J.-F., Matsumoto, K., Montzka, S. A., Raper, S. C. B., Riahi, K., Thomson, A. M., Velders, G. J. M., and van Vuuren, D.: The RCP Greenhouse Gas Concentrations and their Extension from 1765 to 2300, *Climatic Change*, submitted, 2011.

Mitchell, T. D.: Pattern scaling – An examination of the accuracy of the technique for describing future climates, *Climatic Change*, 60, 217–242, 2003.

Monson, R. K., Lipson, D. L., Burns, S. P., Turnipseed, A. A., Delany, A. C., Williams, M. W., and

Estimating the permafrost-carbon feedback

T. Schneider von Deimling
et al.

Title Page

Abstract

Introduction

Conclusions

References

Tables

Figures

◀

▶

◀

▶

Back

Close

Full Screen / Esc

Printer-friendly Version

Interactive Discussion



Schmidt, S. K.: Winter forest soil respiration controlled by climate and microbial community composition, *Nature*, 439, 711–714, 2006.

Moss, R. H., Edmonds, J. A., Hibbard, K. A., Manning, M. R., Rose, S. K., van Vuuren, D. P., Carter, T. R., Emori, S., Kainuma, M., Kram, T., Meehl, G. A., Mitchell, J. F. B., Nakicenovic, N., Riahi, K., Smith, S. J., Stouffer, R. J., Thomson, A. M., Weyant, J. P., and Wilbanks, T. J.: The next generation of scenarios for climate change research and assessment, *Nature*, 463, 7282, doi:10.1038/nature08823, 2010.

Nicolisky, D. J., Romanovsky, V. E., Alexeev, V. A., and Lawrence, D. M.: Improved modeling of permafrost dynamics in a GCM land-surface scheme, *Geophys. Res. Lett.*, 34, L08501, doi:10.1029/2007GL029525, 2007.

O'Connor, F. M., Boucher, O., Gedney, N., Jones, C. D., Folberth, G. A., Coppel, R., Friedlingstein, P., Collins, W. J., Chappellaz, J., Ridley, J., and Johnson, C. E.: Possible role of wetlands, permafrost, and methane hydrates in the methane cycle under future climate change: A review, *Rev. Geophys.*, 48, RG4005, doi:10.1029/2010RG000326, 2010.

Raupach, M., Canadell, J., Dolman, J., Valentini, R., and Freibauer, A.: Observing a Vulnerable Carbon Cycle, in: *The Continental-Scale Greenhouse Gas Balance of Europe*, Springer New York, 5–32, 2008.

Riley, W. J., Subin, Z. M., Lawrence, D. M., Swenson, S. C., Torn, M. S., Meng, L., Mahowald, N. M., and Hess, P.: Barriers to predicting changes in global terrestrial methane fluxes: analyses using CLM4Me, a methane biogeochemistry model integrated in CESM, *Biogeosciences Discuss.*, 8, 1733–1807, doi:10.5194/bgd-8-1733-2011, 2011.

Saito, K., Kimoto, M., Zhang, T., Takata, K., and Emori, S.: Evaluating a high-resolution climate model: Simulated hydrothermal regimes in frozen ground regions and their change under the global warming scenario, *J. Geophys. Res.-Earth*, 112, F02S11, doi:10.1029/2006JF000577, 2007.

Santer, B. D., Wigley, T. M. L., Schlesinger, M. E., and Mitchell, J. F. B.: *Developing Climate Scenarios from Equilibrium GCM Results*, MPI, Hamburg, Germany, 1990.

Scanlon, D. and Moore, T.: Carbon dioxide production from peatland soil profiles: The influence of temperature, oxic/anoxic conditions and substrate, *Soil Science*, 165, 153–160, 2000.

Schaefer, K., Zhang, T., Bruhwiler, L., and Barrett, A. P.: Amount and timing of permafrost carbon release in response to climate warming, *Tellus B*, 63(2), 165–180, 2011.

Schewe, J., Levermann, A., and Meinshausen, M.: Climate change under a scenario near 1.5°C of global warming: monsoon intensification, ocean warming and steric sea level rise,

Estimating the permafrost-carbon feedback

T. Schneider von Deimling
et al.

Title Page

Abstract

Introduction

Conclusions

References

Tables

Figures



Back

Close

Full Screen / Esc

Printer-friendly Version

Interactive Discussion



Earth Syst. Dynam., 2, 25–35, doi:10.5194/esd-2-25-2011, 2011.

Schuur, E. A. G., Bockheim, J., Canadell, J. G., Euskirchen, E., Field, C. B., Goryachkin, S. V., Hagemann, S., Kuhry, P., Laflour, P. M., Lee, H., Mazhitova, G., Nelson, F. E., Rinke, A., Romanovsky, V. E., Shiklomanov, N., Tarnocai, C., Venevsky, S., Vogel, J. G., and Zimov, S. A.: Vulnerability of permafrost carbon to climate change: Implications for the global carbon cycle, *Bioscience*, 58, 701–714, 2008.

Schuur, E. A. G., Vogel, J. G., Crummer, K. G., Lee, H., Sickman, J. O., and Osterkamp, T. E.: The effect of permafrost thaw on old carbon release and net carbon exchange from tundra, *Nature*, 459, 556–559, 2009.

Screen, J. A. and Simmonds, I.: The central role of diminishing sea ice in recent Arctic temperature amplification, *Nature*, 464, 1334–1337, 2010.

Shakhova, N., Semiletov, I., and Gustafsson, O.: Methane from the East Siberian Arctic Shelf Response, *Science*, 329, 1147–1148, 2010a.

Shakhova, N., Semiletov, I., Salyuk, A., Yusupov, V., Kosmach, D., and Gustafsson, O.: Extensive Methane Venting to the Atmosphere from Sediments of the East Siberian Arctic Shelf, *Science*, 327, 1246–1250, 2010b.

Sitch, S., Smith, B., Prentice, I. C., Arneth, A., Bondeau, A., Cramer, W., Kaplan, J. O., Levis, S., Lucht, W., Sykes, M. T., Thonicke, K., and Venevsky, S.: Evaluation of ecosystem dynamics, plant geography and terrestrial carbon cycling in the LPJ dynamic global vegetation model, *Glob. Change Biol.*, 9, 161–185, 2003.

Sitch, S., Huntingford, C., Gedney, N., Levy, P. E., Lomas, M., Piao, S. L., Betts, R., Ciais, P., Cox, P., Friedlingstein, P., Jones, C. D., Prentice, I. C., and Woodward, F. I.: Evaluation of the terrestrial carbon cycle, future plant geography and climate-carbon cycle feedbacks using five Dynamic Global Vegetation Models (DGVMs), *Glob. Change Biol.*, 14, 2015–2039, 2008.

Stroeve, J., Holland, M. M., Meier, W., Scambos, T., and Serreze, M.: Arctic sea ice decline: Faster than forecast, *Geophys. Res. Lett.*, 34, L09501, doi:10.1029/2007GL029703, 2007.

Swann, A. L., Fung, I. Y., Levis, S., Bonan, G. B., and Doney, S. C.: Changes in Arctic vegetation amplify high-latitude warming through the greenhouse effect, *Proceedings of the National Academy of Sciences of the United States of America*, 107, 1295–1300, 2010.

Tarnocai, C., Canadell, J. G., Schuur, E. A. G., Kuhry, P., Mazhitova, G., and Zimov, S.: Soil organic carbon pools in the northern circumpolar permafrost region, *Global Biogeochem. Cy.*, 23, GB2023, doi:10.1029/2008GB003327, 2009.

van Vuuren, D. P., Edmonds, J., Kainuma, M. L. T., Riahi, K., Thomson, A., Matsui, T., Hurtt,

Estimating the permafrost-carbon feedback

T. Schneider von Deimling
et al.

Title Page

Abstract

Introduction

Conclusions

References

Tables

Figures

⏪

⏩

◀

▶

Back

Close

Full Screen / Esc

Printer-friendly Version

Interactive Discussion

G., Lamarque, J.-F., Meinshausen, M., Smith, S., Grainer, C., Rose, S., Hibbard, K. A., Nacicenovic, N., Krey, V., and Kram, T.: Representative Concentration Pathways: an overview, *Climatic Change*, submitted, 2011.

Wagner, D., Liebner, S., and Margesin, R.: Global Warming and Carbon Dynamics in Permafrost Soils: Methane Production and Oxidation, in: *Permafrost Soils*, Springer Berlin Heidelberg, 219–236, 2009.

Walter, B. P. and Heimann, M.: A process-based, climate-sensitive model to derive methane emissions from natural wetlands: Application to five wetland sites, sensitivity to model parameters, and climate, *Global Biogeochem. Cy.*, 14, 745–765, 2000.

Walter, K. M., Zimov, S. A., Chanton, J. P., Verbyla, D., and Chapin, F. S.: Methane bubbling from Siberian thaw lakes as a positive feedback to climate warming, *Nature*, 443, 71–75, 2006.

Walter, K. M., Edwards, M. E., Grosse, G., Zimov, S. A., and Chapin, F. S.: Thermokarst lakes as a source of atmospheric CH₄ during the last deglaciation, *Science*, 318, 633–636, 2007a.

Walter, K. M., Smith, L. C., and Chapin, F. S.: Methane bubbling from northern lakes: present and future contributions to the global methane budget, *Philosophical Transactions of the Royal Society a-Mathematical Physical and Engineering Sciences*, 365, 1657–1676, 2007b.

Wania, R., Ross, I., and Prentice, I. C.: Integrating peatlands and permafrost into a dynamic global vegetation model: 2. Evaluation and sensitivity of vegetation and carbon cycle processes, *Global Biogeochem. Cy.*, 23, GB3014, doi:10.1029/2008GB003413, 2009.

Wigley, T. M. L. and Raper, S. C. B.: Reasons for larger warming projections in the IPCC Third Assessment Report, *J. Climate*, 15, 2945–2952, 2002.

Yi, S. H., Woo, M. K., and Arain, M. A.: Impacts of peat and vegetation on permafrost degradation under climate warming, *Geophys. Res. Lett.*, 34, L16504, doi:10.1029/2007GL030550, 2007.

Zhang, Y., Chen, W. J., and Riseborough, D. W.: Transient projections of permafrost distribution in Canada during the 21st century under scenarios of climate change, *Global Planet. Change*, 60, 443–456, 2008.

Zhuang, Q. L., Melillo, J. M., Sarofim, M. C., Kicklighter, D. W., McGuire, A. D., Felzer, B. S., Sokolov, A., Prinn, R. G., Steudler, P. A., and Hu, S. M.: CO₂ and CH₄ exchanges between land ecosystems and the atmosphere in northern high latitudes over the 21st century, *Geophys. Res. Lett.*, 33, L17403, doi:10.1029/2006GL026972, 2006.

Table 1. Default and sensitivity range parameters of the permafrost module. Sensitivity ranges are sampled from uniform distributions between the stated minimal and maximal value.

Parameter	Description	Unit	Default	Sensitivity Range
Permafrost Module				
N	Number of zonal bands		50	50
T_{\max}	Regional Arctic temperature anomaly threshold for "northernmost" zonal band	°C	10	[8 12]
T_{\min}	Regional Arctic temperature anomaly threshold for "southernmost" zonal band	°C	0	0
β_{ms}	Annual Freezing or Thawing Rate of Mineral Soil Fraction	% °C ⁻¹ yr ⁻¹	0.01	[0.005 0.015]
β_{peat}	Annual Freezing or Thawing Rate of Peatland Soil Fraction	% °C ⁻¹ yr ⁻¹	0.005	[0.0025 0.0075]
α	Amplification of global warming over permafrost area rel. to global mean warming	°C/°C	1.6	[1.4 2]
Φ	Amplitude of Annual Temperature Cycle in upper soil	°C	5	[4 6]
$\tau_{\text{ms,aer}}$	Default turnover time of aerobic mineral soil fraction at 10 °C	ys	40	[30 60]
λ_{an}	Q10 Temperature feedback norm factor for anaerobic decomposition rate	°C	309 (Q10 = 2.3)	[256 662] (Q10 = [2 6])
λ_{aer}	Q10 Temperature feedback norm factor for aerobic decomposition rate	°C	309 (Q10 = 2.3)	[256 513] (Q10 = [2 4])
m_T	Temperature sensitivity of the simplified soilwater parameterisation.	°C ⁻¹	0.04	[0.032 0.048]
W_{offset}	An offset in the simplified soilwater parameterisation	Mass Fraction	0.02	[0.018 0.022]
W_{min}	The minimal soilwater content	Mass Fraction	0.02	[0.018 0.022]
$R_{\text{peat/ms}}$	Ratio of decomposition rate in peatland vs. mineral soil	Fraction	0.5	[0.3 0.7]
$R_{\text{an/aer}}$	Ratio of anaerobic vs. aerobic decomposition rate	Fraction	0.1	[1/40 1/7]
$A_{\text{ms,an}}$	Area fraction of mineral soil with anaerobic decomposition	Fraction	0.05	[0.01 0.1]
$A_{\text{peat,an}}$	Area fraction of peatland soil with anaerobic decomposition	Fraction	0.8	[0.7 0.9]
C_0	The total initial carbon pool	PgC	800	[600 1000]
R_{ms}	Fraction of total carbon that is in mineral soil	Fraction	0.8	[0.7 0.9]
φ	Distribution of total carbon content towards the "Southern" (1) or "Northern" Areas (-1) or uniformly equal distribution (0).		0	[-0.5 0.5]
χ	Fraction of methane oxidation on its transport to the atmosphere	Fraction	0.15	[0.1 0.2]

Estimating the permafrost-carbon feedback

T. Schneider von Deimling
et al.

Title Page

Abstract

Introduction

Conclusions

References

Tables

Figures

◀

▶

◀

▶

Back

Close

Full Screen / Esc

Printer-friendly Version

Interactive Discussion



Estimating the permafrost-carbon feedback

T. Schneider von Deimling
et al.

Title Page

Abstract

Introduction

Conclusions

References

Tables

Figures



Back

Close

Full Screen / Esc

Printer-friendly Version

Interactive Discussion



Table 2. Median (68 %-range) estimates of permafrost characteristics under the four RCPs in yr 2100, 2200 and 2300. The thawed permafrost area is provided, weighted in relation to the initial carbon pool distribution. Cumulative emissions of CO₂, CH₄ and the share of carbon that is released as methane are shown for cumulative emissions from pre-industrial times until the indicated year. Subsequent rows indicate additional CO₂ concentrations, CO₂ radiative forcing, CH₄ radiative forcing and global mean temperatures due to permafrost thawing above the background scenario. The permafrost carbon sensitivity γ_{LP} indicates the change in the permafrost carbon stock until that year, given relative to that year's global mean surface temperature.

RCP3-PD	2100	2200	2300
Thawed Permafrost (%)	15% (11–22%)	20% (15–29%)	21% (15–30%)
Cumulative CO ₂ Emissions (PgC)	4 (2–7)	10 (5–19)	15 (8–29)
Cumulative CH ₄ Emissions (MtCH ₄)	155 (71–337)	469 (209–1032)	808 (355–1746)
Carbon released as Methane (%)	3% (1–6%)	3% (2–6%)	4% (2–7%)
Added CO ₂ Concentration (ppm)	1 (1–2)	2 (1–5)	3 (2–6)
Delta CO ₂ Radiative Forcing (W m ⁻²)	0.01 (0.01–0.03)	0.03 (0.02–0.07)	0.05 (0.02–0.09)
Delta CH ₄ Radiative Forcing (W m ⁻²)	0 (0–0.01)	0 (0–0.01)	0 (0–0.01)
Delta Temperature (°C)	0.01 (0–0.02)	0.02 (0.01–0.05)	0.03 (0.01–0.07)
Permafrost Carbon Sensitivity γ_{LP} (PgC/°C)	2.4 (1.4–4)	7.4 (4.5–12)	13 (8–20.7)
RCP45			
Thawed Permafrost (%)	23% (16–33%)	38% (27–54%)	44% (32–63%)
Cumulative CO ₂ Emissions (PgC)	8 (4–15)	32 (16–66)	60 (30–124)
Cumulative CH ₄ Emissions (MtCH ₄)	227 (101–506)	988 (438–2200)	2060 (877–4593)
Carbon released as Methane (%)	2% (1–4%)	2% (1–4%)	3% (1–4%)
Added CO ₂ Concentration (ppm)	2 (1–5)	10 (4–22)	18 (8–39)
Delta CO ₂ Radiative Forcing (W m ⁻²)	0.02 (0.01–0.05)	0.09 (0.04–0.2)	0.17 (0.08–0.34)
Delta CH ₄ Radiative Forcing (W m ⁻²)	0.01 (0–0.01)	0.01 (0–0.02)	0.01 (0–0.02)
Delta Temperature (°C)	0.02 (0.01–0.04)	0.07 (0.03–0.16)	0.12 (0.05–0.29)
Permafrost Carbon Sensitivity γ_{LP} (PgC/°C)	2.9 (1.7–5)	11.2 (6.6–18.5)	20 (11.8–32.1)
RCP6			
Thawed Permafrost (%)	26% (18–38%)	57% (41–82%)	69% (50–96%)
Cumulative CO ₂ Emissions (PgC)	9 (5–19)	68 (34–143)	138 (71–280)
Cumulative CH ₄ Emissions (MtCH ₄)	245 (110–548)	1647 (720–3884)	3776 (1652–9157)
Carbon released as Methane (%)	2% (1–4%)	2% (1–3%)	2% (1–4%)
Added CO ₂ Concentration (ppm)	3 (2–7)	25 (11–55)	49 (22–103)
Delta CO ₂ Radiative Forcing (W m ⁻²)	0.03 (0.01–0.05)	0.17 (0.08–0.34)	0.32 (0.16–0.62)
Delta CH ₄ Radiative Forcing (W m ⁻²)	0.01 (0–0.02)	0.02 (0.01–0.05)	0.02 (0.01–0.05)
Delta Temperature (°C)	0.02 (0.01–0.05)	0.13 (0.06–0.33)	0.24 (0.11–0.6)
Permafrost Carbon Sensitivity γ_{LP} (PgC/°C)	2.8 (1.6–4.9)	16.1 (9.1–25.9)	29.6 (17.8–45.1)
RCP85			
Thawed Permafrost (%)	46% (31–66%)	98% (90–100%)	100% (99–100%)
Cumulative CO ₂ Emissions (PgC)	26 (12–52)	320 (170–543)	529 (362–705)
Cumulative CH ₄ Emissions (MtCH ₄)	493 (212–1198)	6393 (2622–16571)	16964 (7440–41289)
Carbon released as Methane (%)	1% (1–3%)	2% (1–3%)	3% (1–5%)
Added CO ₂ Concentration (ppm)	10 (4–22)	113 (59–239)	181 (98–331)
Delta CO ₂ Radiative Forcing (W m ⁻²)	0.05 (0.02–0.11)	0.32 (0.18–0.57)	0.47 (0.28–0.73)
Delta CH ₄ Radiative Forcing (W m ⁻²)	0.01 (0.01–0.03)	0.08 (0.03–0.17)	0.08 (0.03–0.14)
Delta Temperature (°C)	0.05 (0.02–0.11)	0.40 (0.17–0.94)	0.58 (0.3–1.15)
Permafrost Carbon Sensitivity γ_{LP} (PgC/°C)	5.1 (2.7–8.6)	32.1 (21.5–43.3)	46.9 (35.2–61)

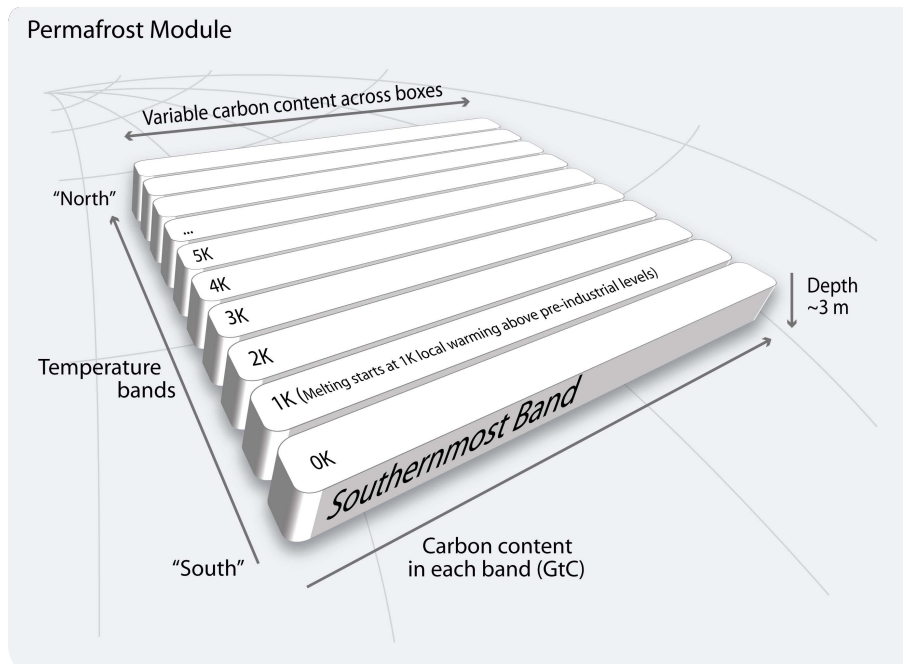


Fig. 1. Schematic overview of the simplified permafrost module with n zonal bands (default $n = 50$) in which thawing starts at different global warming levels. The carbon content of the represented permafrost fractions (approximating upper 3 m soil layer) can vary across the different zonal bands of equally spaced temperature intervals (default = 0.2 K spacing), with the default being an initially uniform carbon content distribution. Each zonal band is further subdivided into four soil pools with differing thaw and decomposition characteristics: mineral and peatland soils, divided into aerobic and anaerobic fractions.

Estimating the permafrost-carbon feedback

T. Schneider von Deimling et al.

Title Page

Abstract

Introduction

Conclusions

References

Tables

Figures

⏪

⏩

◀

▶

Back

Close

Full Screen / Esc

Printer-friendly Version

Interactive Discussion

Estimating the permafrost-carbon feedback

T. Schneider von Deimling
et al.

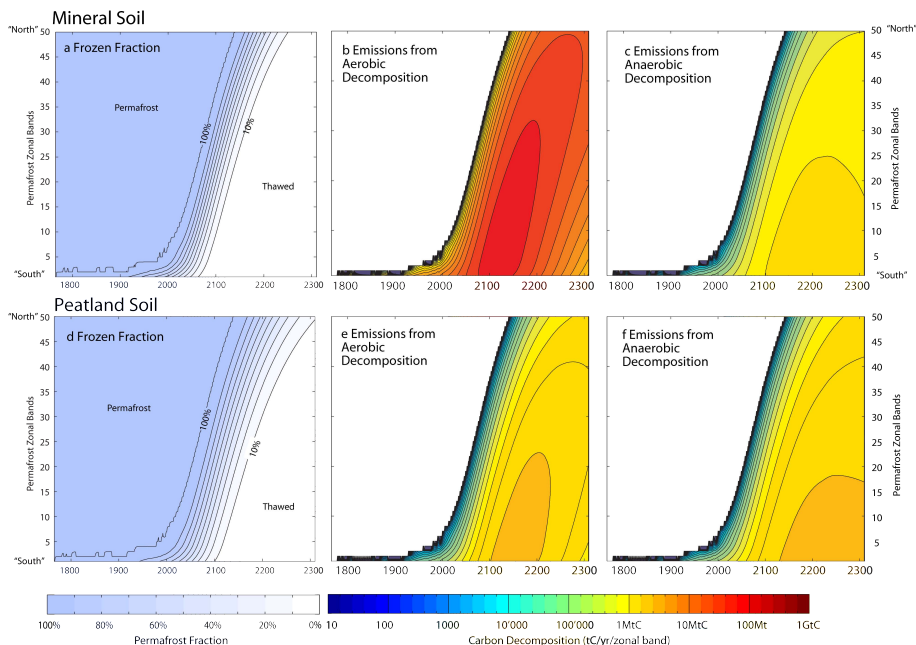


Fig. 2. Fraction of intact permafrost and carbon release in PgC yr^{-1} per zonal band from mineral soil (upper row) and peatland soil (lower row) via aerobic (**b, e**) and anaerobic (**c, f**) decomposition, respectively, under the RCP8.5 scenario and illustrative default settings (see text and Table 2). Starting in the “Southernmost” zonal band, the thawing of the parameterized 3 m thick soil layer progresses northward to colder zonal bands (vertical axis) over time (horizontal axis) (see panel **a, d**), being followed by carbon releases.

Title Page

Abstract

Introduction

Conclusions

References

Tables

Figures

⏪

⏩

◀

▶

Back

Close

Full Screen / Esc

Printer-friendly Version

Interactive Discussion

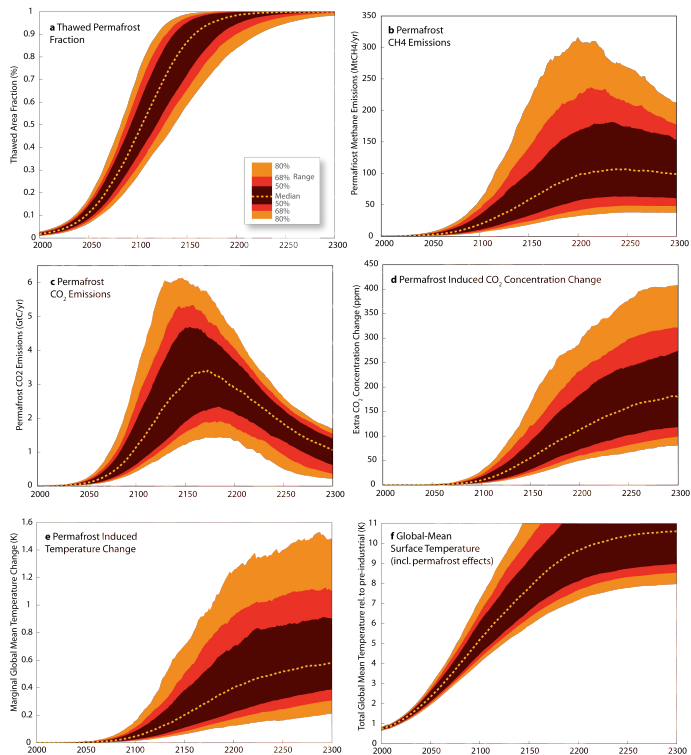


Fig. 3. This study's estimated ranges of thawed permafrost fraction (a), permafrost methane (b) and CO₂ emissions (c), permafrost induced CO₂ concentration (d) and temperature change (e), and the total anthropogenically induced global mean temperature anomaly (f). Results were obtained from an uncertainty analysis for the RCP8.5 scenario. The uncertainty ranges result from 600 member ensemble simulations, using a Monte Carlo sampling that combines the joint distribution of 82 climate model parameters, 9 sets of 17 carbon cycle parameters and 21 independently sampled parameters of our permafrost model (see text and Table 2).

Estimating the permafrost-carbon feedback

T. Schneider von Deimling et al.

Title Page

Abstract Introduction

Conclusions References

Tables Figures

◀ ▶

◀ ▶

Back Close

Full Screen / Esc

Printer-friendly Version

Interactive Discussion



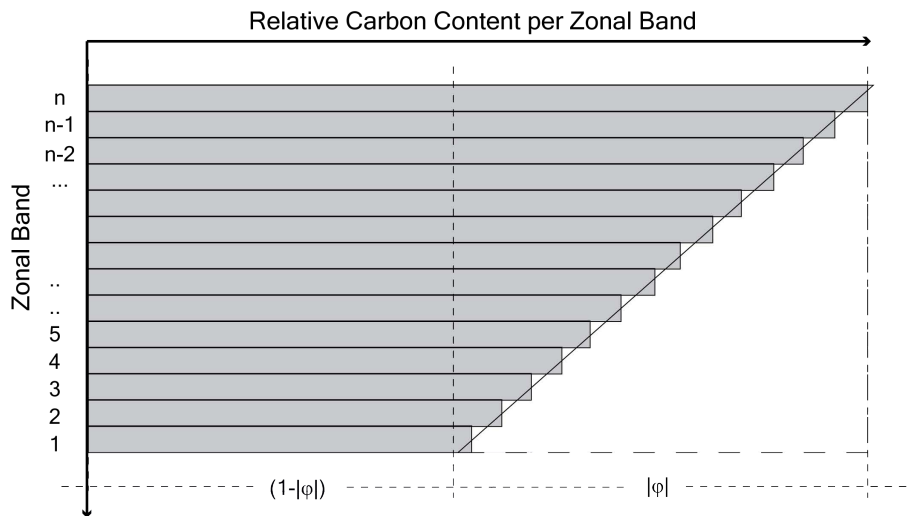


Fig. A1. Illustration of the simplified parameterisation to vary the north-south distribution of the initial carbon content C_0 across the n zonal bands with the parameter φ , here shown for a “northward” bias ($-1 < \varphi < 0$). By default ($\varphi = 0$), each zonal band is allocated the same share, $1/n C_0$.

Estimating the permafrost-carbon feedback

T. Schneider von Deimling et al.

Title Page

Abstract Introduction

Conclusions References

Tables Figures

⏪ ⏩

◀ ▶

Back Close

Full Screen / Esc

Printer-friendly Version

Interactive Discussion

